

N 7 8 1 0 6 5 6

**NASA TECHNICAL
MEMORANDUM**

NASA TM X-68150

NASA TM X-68150

**CASE FILE
COPY**

**ENERGY DISTRIBUTION FUNCTIONS OF KILOVOLT IONS
IN A MODIFIED PENNING DISCHARGE**

by J. Reece Roth
Lewis Research Center
Cleveland, Ohio

TECHNICAL PAPER proposed for presentation at
Fourteenth Annual Meeting of the Plasma Physics Division
of the American Physical Society
Monterey, California, November 13-16, 1972

ENERGY DISTRIBUTION FUNCTIONS OF KILOVOLT IONS
IN A MODIFIED PENNING DISCHARGE

by J. Reece Roth

Lewis Research Center
National Aeronautics and Space Administration
Cleveland, Ohio

ABSTRACT

The distribution function of ion energy parallel to the magnetic field of a modified Penning discharge has been measured with a retarding potential energy analyzer. These ions escaped through one of the throats of the magnetic mirror geometry. Simultaneous measurements of the ion energy distribution function perpendicular to the magnetic field have been made with a charge-exchange neutral detector. The ion energy distribution functions are approximately Maxwellian, and the parallel and perpendicular kinetic temperatures are equal within experimental error. These results suggest that turbulent processes previously observed in this discharge Maxwellianize the velocity distribution along a radius in velocity space, and result in an isotropic energy distribution. The kinetic temperatures observed are on the order of kilovolts, and the tails of the ion energy distribution functions are Maxwellian for up to a factor of 7 e-folds in energy. When the distributions depart from Maxwellian, they are enhanced above the Maxwellian tail. Above densities of about 10^{10} particles per cubic centimeter, this enhancement appears to be the result of a second, higher temperature Maxwellian distribution. At these high particle energies, only the ions perpendicular to the magnetic field lines were investigated.

INTRODUCTION

Previous investigations of a modified Penning discharge by Roth (1966) revealed ions with approximately Maxwellian velocity distributions and kilovolt kinetic temperatures. The diagnostic instrument used to measure the energy distribution of ions parallel to the magnetic field lines was a retarding potential analyzer located outside one of the magnetic mirrors. The data reduction procedures and experimental results from an extensive series of measurements with the retarding potential energy analyzer were reported by Roth and Clark (1969).

In view of the possible application of the modified Penning discharge to a steady-state plasma heating scheme for fusion research, it is desirable to independently confirm the high ion kinetic temperatures and Maxwellian velocity distribution observed in the ions lost along the magnetic field lines. The present investigation reports a comparison in which the parallel and perpendicular ion energy distribution functions were simultaneously measured for 163 experimental runs taken under a range of operating conditions. Such simultaneous measurements have not been reported in the literature of Penning discharges, although Konstantinov et al. (1972) have measured the energy of charge-exchange neutrals from the midplane of a modified Penning discharge. In the present investigation, a charge-exchange neutral detector is used to measure the perpendicular ion energy, while simultaneous observations of the parallel ion energy are made with the retarding potential energy analyzer.

Characteristics of Modified Penning Discharge

The operating characteristics of the discharge have been described by Roth (1966, 1971); a detailed description of the superconducting mag-

net facility in which the discharge is operated is described by Roth et al. (1965); and some of the physical processes responsible for ion heating are discussed by Roth (1972). An isometric cutaway drawing of the experimental configuration is shown in Figure 1. The plasma is approximately 15 cm in diameter at the midplane. The magnetic field consists of a magnetic mirror with a 2.62:1 mirror ratio generated by two superconducting coils, the dewars of which are approximately 18 cm in diameter at the magnetic mirror throats. The magnet system shown in Figure 1 is located in a vacuum tank 1 meter in diameter and approximately 2 meters long, giving very good experimental and visual access to the experimental volume. The parallel dewars on either side of the experimental volume are at liquid nitrogen temperature. The anode ring is operated at positive potentials up to 35 kV with respect to the walls of the vacuum tank and the electrical circuit to the power supply is completed by ions which impinge on the grounded tank walls.

The experimental investigation consists of 163 runs taken with deuterium gas. The maximum value of the magnetic field was 1 tesla at the magnetic mirror throats and 0.38 tesla at the midplane, in the vicinity of the anode rings. From previous measurements taken with a Langmuir probe at the throat of the mirror (Roth 1972), the electron temperature is known to be approximately 50 eV, within a factor of 2, in this plasma. This is as much as an order of magnitude below the ion temperature at the same operating conditions. Any atomic deuterium generated in the plasma volume has ample opportunity to recombine on the walls before it can return to the experimental volume, as a result of the long mean

free paths for binary collision processes. Because of the rather large vacuum tank wall area and the cold liquid nitrogen surfaces on either side of the plasma volume, it is unlikely that a significant population of atomic deuterium can exist in the plasma. For this reason it was assumed that the neutral background gas consisted of molecular deuterium gas. The principal ionized species within the plasma was taken to be ionized deuterium atoms D^+ . It is believed that D^+ dominated the plasma because investigation of the spectrum of electrostatic potential fluctuations yielded a peak at the ion cyclotron frequency of D^+ (when such a peak could be observed) and peaks were absent or much fainter by comparison at the ion cyclotron frequency appropriate to ionized molecular deuterium, D_2^+ .

The 163 experimental runs spanned a range of the positive anode voltage from 5 kV to 35 kV, and neutral background pressures, p_0 , from 3.9×10^{-5} to 12.0×10^{-5} torr, where the neutral deuterium pressure has been corrected for the gage factor of this apparatus. It is estimated from previous work (Roth, 1972) that the ion density at the midplane of the modified Penning discharge ranged from approximately 10^9 to 6×10^{10} particles per cubic centimeter in this investigation.

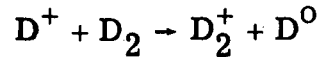
Diagnostic Instruments

The ion energy distribution function was measured by two non-perturbing diagnostic techniques, one parallel to the magnetic field lines, and the other perpendicular to the magnetic field lines. In Figure 2(a) is a schematic drawing of the retarding potential energy analyzer used to measure the parallel distribution function of ions leaving the plasma

through the magnetic mirror throat. The analyzer was located approximately 20 cm outside the magnetic mirror throat and 10 cm from the magnetic axis. The analyzer was parallel to the local magnetic field line and measured the parallel component of the ion energy. The raw data, taken on an X-Y recorder, represents an integrated ion energy distribution function. A computer program determines, by iteration, the integrated Maxwellian distribution which best fits the raw data, in the sense of minimizing the mean square error between the logarithms of the best fitting distribution and of the raw data. Using the logarithm of the value of the data point rather than the actual value of the data point tended to give approximately equal weight to all portions of the data curves. By comparing the best fitting computer solution to the raw data, one may assess the extent to which the raw data are Maxwellian by observing the extent to which the best-fitting curve is also a good fit. The principal source of error for this application of the retarding potential energy analyzer is in the iterative procedure used to reduce the data, which sometimes does not converge to the proper kinetic temperature (this was determined by obtaining a best fit to "pseudo-data," an integrated Maxwellian of specified kinetic temperature). These convergence problems give rise to errors in the parallel ion kinetic temperature which may be as high as twenty percent. The analytical theory, error analysis, and experimental application of the retarding potential energy analyzer have been discussed by Roth and Clark (1969).

The charge-exchange neutral detector used in these investigations is a geometric duplicate of that developed at Fontenay-aux-Roses (Valckx 1964). The particle detector electronic system was developed at the NASA Lewis Research Center. A schematic of this instrument and its location with respect to the plasma is indicated on Figure 2(b). The retarding potential energy analyzer and the neutral detector were positioned to sample the anode sheath, approximately 1 cm from the inner circumference of the anode ring. Fast ions in the sheath between the plasma and the anode ring charge exchange on the background of neutral molecular deuterium gas, and the resulting fast deuterium atoms then move along straight lines to the walls of the vacuum vessel. In the neutral detector, some of the fast neutrals pass through a series of slits and are reionized by a nitrogen gas cell, which is maintained at pressures of approximately 100 microns. The reionized fast particles then pass through additional focusing slits into a set of 90° electrostatic deflector plates. The energy of the ions which may pass through the 90° deflector plates is determined by the potential applied across them. By changing the voltage applied between the deflector plates, one may sweep out the energy distribution function of the reionized particles. The ions are passed through a second series of slits and impinge on a photomultiplier detector, which counts individual particles.

The particle flux at the photomultiplier is only indirectly related to the ion distribution function inside the confined plasma. To obtain the original ion distribution function, one must correct for the charge exchange process of atomic deuterium ions on molecular deuterium,



One must also correct for the reionization cross-section in the nitrogen gas cell, and for the energy resolution of the electrostatic analyzer.

The flux $I(V)$ of individual particles reaching the photomultiplier may be written

$$I(V) = C_0 n_i n_0 \sigma_x(V) v_i f(V) k(V) G_a(V) \quad (1)$$

where V is the ion energy in electron volts, C_0 is a geometrical and dimensional constant, $f(V)$ is the desired ion energy distribution, $k(V)$ is the reionization probability of atomic deuterium in a nitrogen gas cell and is given by Barnett, et al. (1964), $G_a(V)$ is a correction for the energy resolution of the analyzer, and results from the fact that the relative energy resolution, dV/V , is independent of energy. Thus, the energy resolution involves correction by a factor

$$G_a(V) \sim V \quad (2)$$

The factor $n_i n_0 \sigma_x(V) v_i$ is the number of charge exchange reactions/cm³-sec in the volume sampled by the analyzer, n_i and n_0 are the ion and neutral number density, respectively, and v_i is the deuterium ion velocity. The charge exchange cross section $\sigma_x(V)$ is available in

Barnett, et al. (1964), and is known from $70 \text{ eV} \leq V \leq 200 \text{ keV}$. The correction factor $k(V)$ for the nitrogen gas cell is known for energies over the range $2 \leq V \leq 100 \text{ keV}$, and is

$$k(V) \sim V^{0.56} \quad (3)$$

over this range Valckx (1964), Barnett et al. (1964).

One may convert the raw data for $I(V)$ to the distribution function of ion energy in the plasma, $f(V)$ by using Eqs. (1) to (3) to obtain

$$f(V) = \frac{C_1 I(V)}{V^{2.06} \sigma_X(V)} \quad (4)$$

where C_1 is a constant for the apparatus. The ion energy distribution function obtained from Eq. (4) was used as input to a computer program which obtained a Maxwellian distribution with a least squares best fit to the experimentally determined ion energy distribution $f(V)$. Because the correction factor, $k(V)$, was not known for nitrogen gas below 2 kV, raw data below 2 kV were not utilized in obtaining the best fitting Maxwellian distribution. The principal error in applying the neutral detector arose from establishing the zero level and rounding off errors in reading the raw data. These errors, combined with uncertainties in the charge-exchange cross-sections, may have introduced an error of as much as 10 percent in determining the perpendicular ion kinetic temperature.

EXPERIMENTAL RESULTS

In Figure 3 is shown a characteristic example of data which were taken simultaneously with the retarding potential energy analyzer and the charge exchange neutral detector. The anode voltage was 8 kV, and the neutral background gas pressure was 5.2×10^{-5} torr of deuterium. Figure 3(a) is the energy distribution function measured with the charge exchange neutral detector, corrected with Eq. (4), and plotted as a function of energy on a semi-logarithmic graph. The corrected raw data are indicated by the round symbols and the Maxwellian distribution which best fits this raw data is indicated by the triangular symbols. In Figure 3(b) is shown the integrated energy distribution function measured with the retarding potential energy analyzer. The round symbols are the raw data and the triangular symbols are the best fitting integrated Maxwellian distribution. Figure 3(a) gives a perpendicular component of the ion kinetic temperature, $V_{\perp} = 620$ eV, and Figure 3(b) a best-fitting parallel kinetic temperature, $V_{\parallel} = 559$ eV. It is characteristic in Figure 3 that both the parallel and perpendicular ion energy distribution functions are approximately Maxwellian, that the Maxwellian tail of the neutral detector data extends over approximately 7 e-folding lengths in energy, and that the parallel and perpendicular ion energies are approximately equal within the scatter in the data of the two diagnostic methods employed.

In Figure 4 is a second example of the perpendicular and parallel ion energy spectra, under conditions which yielded kinetic temperatures

of nearly 2 kilovolts. The operating conditions were an anode voltage of 35 kV, and a neutral background gas pressure of 4.3×10^{-5} torr of deuterium. In Figure 4(a) is the neutral detector spectrum with a best-fitting perpendicular kinetic temperature of $V_{\perp} = 1942$ eV. In Figure 4(b) is the retarding potential data, with a best-fitting parallel kinetic temperature of $V_{\parallel} = 1705$ eV. The knee on the latter data indicates that the magnetic field line on which the retarding potential analyzer was located was floating at a positive potential of $V_f = 2200$ volts, an unusually high value for this experiment, but only 6 percent of the applied anode voltage. Figures 3 and 4 are characteristic in that, due to instrumental limitations, it was possible to take valid data at higher ion energies with the neutral detector than with the retarding potential energy analyzer.

Ion energy distributions analogous to those shown in Figures 3 and 4 were obtained for all 163 runs. Kinetic temperatures obtained from the best-fitting Maxwellian distributions are shown in Figure 5. On the small number of occasions for which a two-temperature Maxwellian distribution was observed with the neutral detector, the lowest of the two kinetic temperatures was plotted in Figure 5. On the abscissa is the kinetic temperature derived from the parallel component of ion energy, measured with the retarding potential energy analyzer. On the ordinate is the kinetic temperature derived from the perpendicular component of ion energy measured with the charge exchange neutral detector. There is approximate agreement of the parallel and perpendicular components of the ion kinetic temperature over the range of data taken.

The agreement of V_{\perp} with V_{\parallel} , and the degree of data spread may be estimated by fitting the data in Figure 5 to the relation

$$V_{\perp} = C_2 V_{\parallel} \quad (5)$$

and obtaining the median and relative standard deviation of C_2 . In Figure 6, the cumulative probability of C_2 for 163 runs is plotted on probability graph paper. The author's best estimate of the Gaussian distribution to the data is indicated by the straight line. The median value of C_2 , $\overline{C_2}$, is the intersection of the the best-fitting straight line with the 50 percent line.

$$\overline{C_2} = 1.04 \quad (6)$$

which implies that the perpendicular energy is slightly higher than the parallel energy. The relative standard deviation of the data population, the horizontal distance between the intersection of the best-fitting straight line with the median and the one standard deviation lines, was approximately

$$\Delta C_2 = \frac{\delta(C_2)}{\overline{C_2}} = 0.26 \quad (7)$$

Thus, the parallel and perpendicular ion kinetic temperatures are equal to within the estimated experimental error. The parameter C_2 was plotted as a function of the independent variables (anode voltage and neutral gas pressure) for the 163 runs, and no systematic trend of C_2 was observed. The same physical process which is responsible for making C_2 a fixed constant apparently operates over the entire range of parameters investigated.

Two general types of anomalous ion energy distributions were observed in the perpendicular ion energy distribution function. Both were characterized by an increase of the observed distribution function above the best fitting Maxwellian value in the tail of the distribution. This enhancement of the Maxwellian tail assumed two forms. One of these was a two-temperature Maxwellian distribution, in which the Maxwellian tail was dominated by a hotter component of lower density, giving the type of ion energy distribution function illustrated in Figure 7. Two temperature distributions were observed only at plasma densities above approximately 10^{10} particles per cubic centimeter. This two temperature Maxwellian distribution apparently results from the analyzer sampling two separate regions with different ion kinetic temperatures.

Two temperature Maxwellian distributions may also occur as a result of a population of hot impurities superimposed on the distribution function of the principal species. Such impurities, with each species having a distinct ion temperature, have been described by Stirling (1972). This explanation is unsatisfactory for the present experiment, however, since observation of the Penning discharge plasma with a bench spectrometer revealed no detectable impurity lines. Ion energy distributions similar to Figure 7 have been reported by Artsimovich (1972) in connection with the Tokamak series of experiments. Artsimovich reported that two-temperature Maxwellian distributions occurred in the Tokamak at number densities below 10^{12} particles/cm³.

A second anomalous departure from the Maxwellian distribution was observed in approximately a dozen cases, at higher neutral gas pressures. This departure is illustrated in Figure 8 and shows an ion energy distribution function with a bump on the Maxwellian tail at an energy which roughly corresponds to the voltage applied to the anode ring. Such a distribution function may be due to physical processes in the weak plasma penumbra which surrounds the modified Penning discharge.

DISCUSSION AND CONCLUSIONS

The present investigation has demonstrated generally good agreement between the parallel and perpendicular kinetic temperatures observed with non-perturbing diagnostics in a modified Penning discharge. These observations provide an independent confirmation of the results reported by Roth and Clark (1969), in which a sophisticated data reduction procedure was applied to raw data obtained from the modified Penning discharge with a retarding potential energy analyzer. The Maxwellian ion energy distributions observed in the distribution functions parallel and perpendicular to the magnetic field are consistent with a model in which the turbulent processes described by Roth (1971) tend to Maxwellianize the distribution function along a radius in velocity space, such that the ion energy is isotropic in velocity space.

The modified Penning discharge has been shown to be capable of generating a steady-state plasma of kilovolt ion energies and with an energy distribution function that is Maxwellian and virtually isotropic in velocity space. The modified Penning discharge may therefore be of

interest in controlled fusion experiments, particularly in those toroidal systems in which one desires to create an approximately isotropic distribution of hot ions.

ACKNOWLEDGEMENT

R. P. G. Valckx and A. Bariaud of Fontenay-Aux-Roses provided useful conversations and assistance with the construction of the fast neutral energy analyzer.

REFERENCES

1. L. A. Artsimovich, Nucl. Fusion 12, 215 (1972).
2. C. F. Barnett, J. A. Ray and J. C. Thompson, Oak Ridge National Lab. Rep. ORNL-3113, Rev. (1964).
3. S. G. Konstantinov, O. K. Myskin, A. F. Sorokin and F. A. Tsel'nik, Soviet Phys. -Tech. Phys. 16, 2006 (1972).
4. J. R. Roth, D. C. Freeman, Jr. and D. A. Haid, Rev. Sci. Inst. 36, 1481 (1965).
5. J. R. Roth, Rev. Sci. Inst. 37, 1100 (1966).
6. J. R. Roth and M. Clark, Plasma Phys. 11, 131 (1969).
7. J. R. Roth, Phys. Fluids 14, 2193 (1971).
8. J. R. Roth, NASA TN D-6985 (1972).
9. W. L. Stirling, Phys. Fluids 15, 688 (1972).
10. F. P. G. Valckx, NASA TT F-11458 (1968).

FIGURE CAPTIONS

Figure 1. - Isometric cutaway drawing of the modified Penning discharge and the superconducting magnetic mirror facility. The approximate location of the retarding potential energy analyzer, and of the fast neutral energy analyzer are shown schematically.

Figure 2. - Apparatus for measurement of the parallel and perpendicular ion energy distribution functions.

- (a) Retarding potential energy analyzer, located approximately 4 cm from the plasma axis and 20 cm outside the magnetic mirror throat.
 - (b) Schematic drawing of the charge-exchange neutral detector. The line of sight of the detector was tangent to the sheath between the plasma and the anode ring approximately 6 cm below the magnetic axis.
-

Figure 3. - Example of the parallel and perpendicular Maxwellian ion energy distribution functions measured with the instruments shown on Figure 2 for an anode voltage of 8 kV and a deuterium gas pressure of 5.2×10^{-5} torr. On each graph is shown the measured data, and the Maxwellian distribution which best fits the measured data.

- (a) The ion energy distribution function perpendicular to the magnetic field as measured with the charge exchange neutral detector, with $V_{\perp} = 620$.
 - (b) The ion energy distribution function parallel to the magnetic field measured with the retarding potential energy analyzer, with $V_{\parallel} = 559$ eV.
-

Figure 4. - Same as Figure 3, with an anode voltage of 35 kV, and a deuterium gas pressure of 4.3×10^{-5} torr.

(a) Charge exchange neutral detector data with $V_{\perp} = 1942$ eV.

(b) Retarding potential energy analyzer data with $V_{\parallel} = 1706$ eV.

Figure 5. - The parallel and perpendicular ion kinetic temperatures determined from the neutral detector and the retarding potential energy analyzer for the 163 experimental runs.

Figure 6. - Cumulative probability of observing the value of C_2 from Eq. (5) for the population of 163 experimental runs.

Figure 7. - Example of a two-temperature Maxwellian distribution observed with the neutral detector at ion number densities above about $10^{10}/\text{cm}^3$, taken at an anode voltage of 10 kV, and a background pressure of 7.8×10^{-5} torr of deuterium gas.

Figure 8. - Example of an ion energy distribution function measured with the neutral detector with a bump on the Maxwellian tail, taken at an anode voltage of 11 kV, and a background pressure of 1.17×10^{-4} torr of deuterium gas.

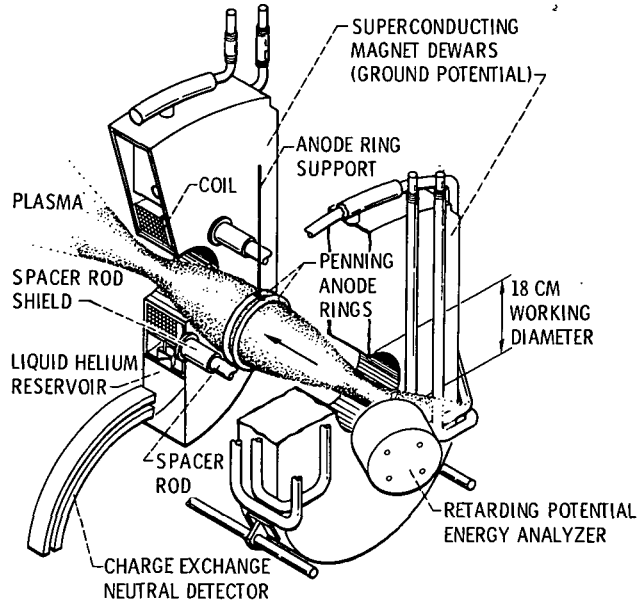


Figure 1

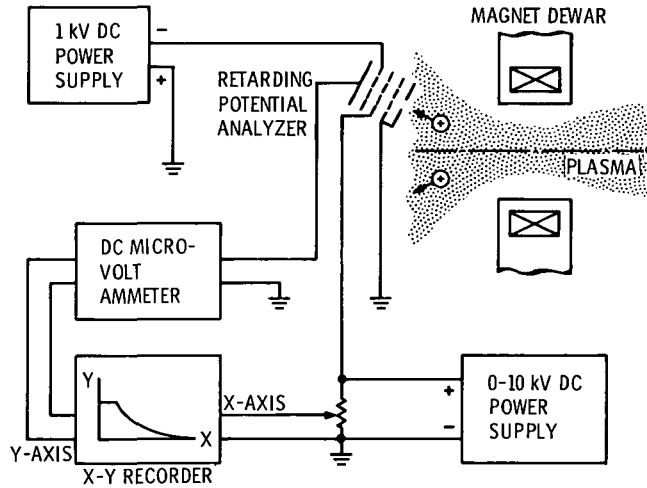


Figure 2(a). - Retarding potential energy analyzer.

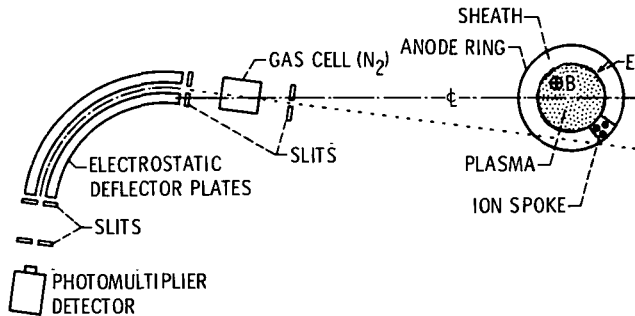
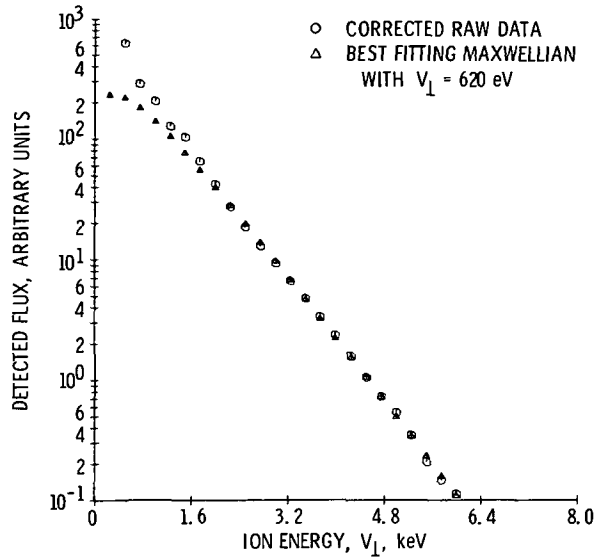
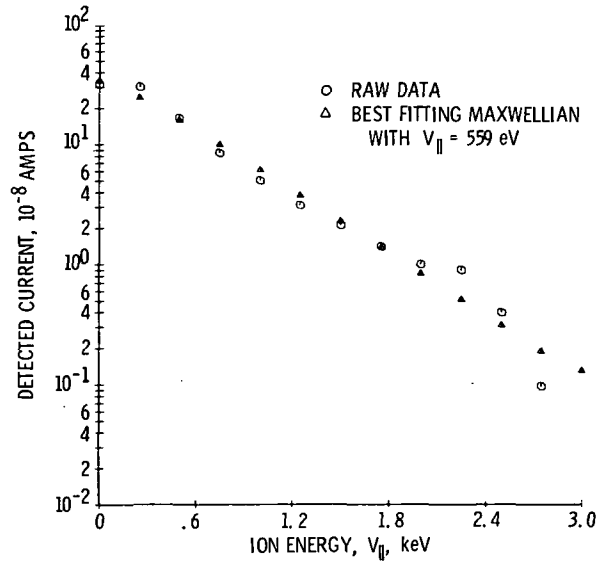


Figure 2(b). - Charge-exchange neutral detector.

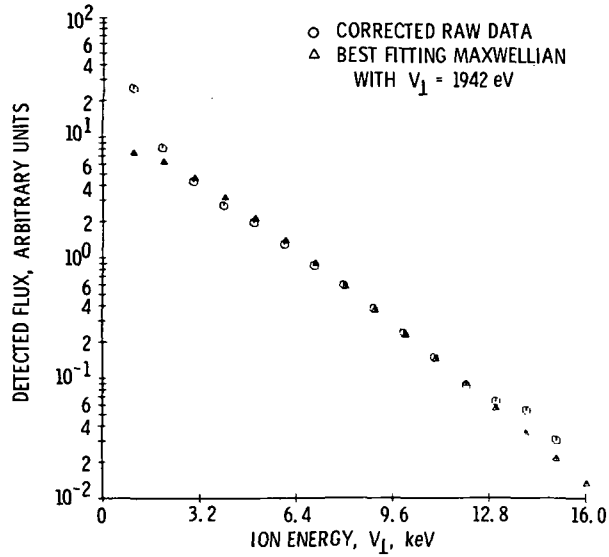


(a) THE ION ENERGY DISTRIBUTION FUNCTION PERPENDICULAR TO THE MAGNETIC FIELD AS MEASURED WITH THE CHARGE EXCHANGE NEUTRAL DETECTOR, WITH $V_{\perp} = 620$.

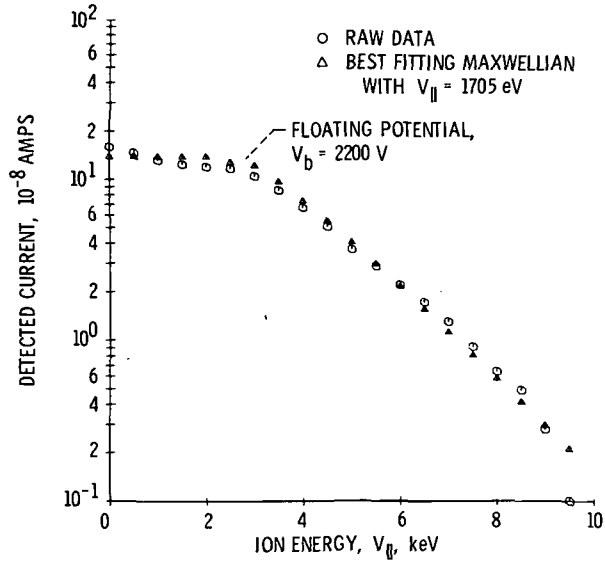


(b) THE ION ENERGY DISTRIBUTION FUNCTION PARALLEL TO THE MAGNETIC FIELD MEASURED WITH THE RETARDING POTENTIAL ENERGY ANALYZER, WITH $V_{\parallel} = 559$ eV.

Figure 3. - Example of the parallel and perpendicular Maxwellian ion energy distribution functions measured with the instruments shown on figure 2 for an anode voltage of 8 kV and a deuterium gas pressure of 5.2×10^{-5} torr. On each graph is shown the measured data, and the Maxwellian distribution which best fits the measured data.



(a) CHARGE EXCHANGE ENERGY ANALYZER DATA WITH $V = 1942$ eV.



(b) RETARDING POTENTIAL DATA WITH $V_{||} = 1706$ eV.

Figure 4. - Same as figure 3, with an anode voltage of 35 kV, and a deuterium gas pressure of 4.3×10^{-5} torr.

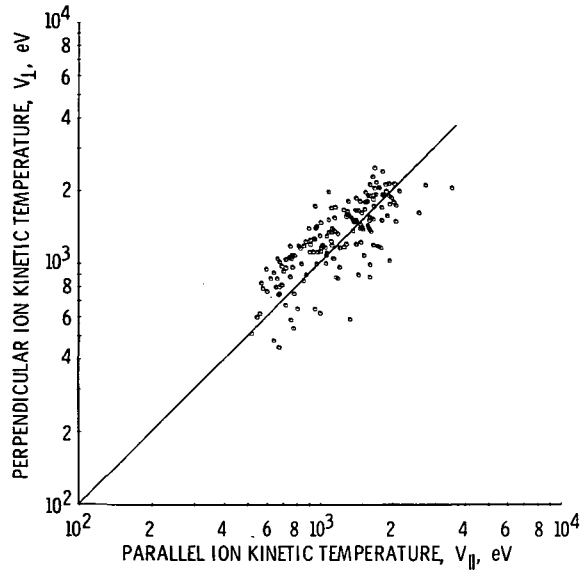


Figure 5. - The parallel and perpendicular ion kinetic temperature determined from the neutral detector and the retarding potential energy analyzer for the 163 experimental runs.

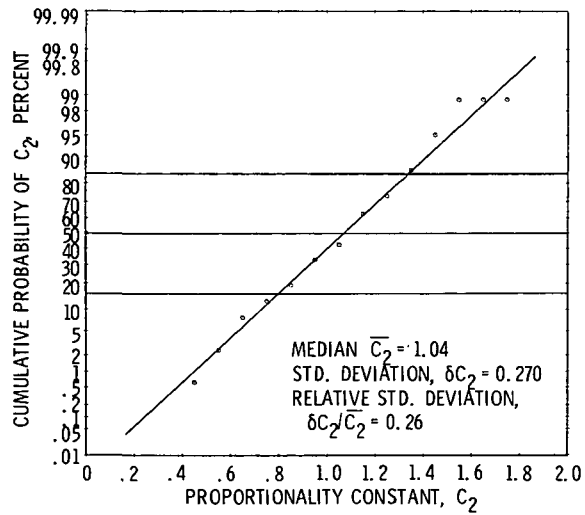


Figure 6. - Cumulative probability of observing the value of C_2 from equation (5) for the population of 163 experimental runs.

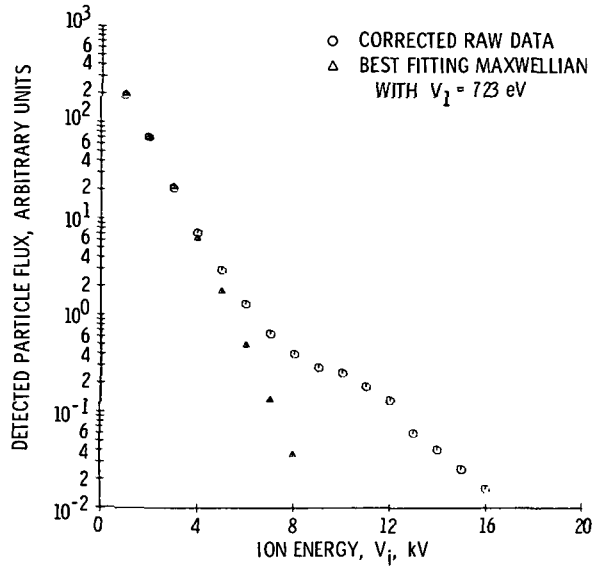


Figure 7. - Example of a two-temperature Maxwellian distribution observed with the neutral detector at ion number densities above about $10^{10}/\text{cm}^3$, taken at an anode voltage of 10 kV, and a background pressure of 7.8×10^{-5} torr of deuterium gas.

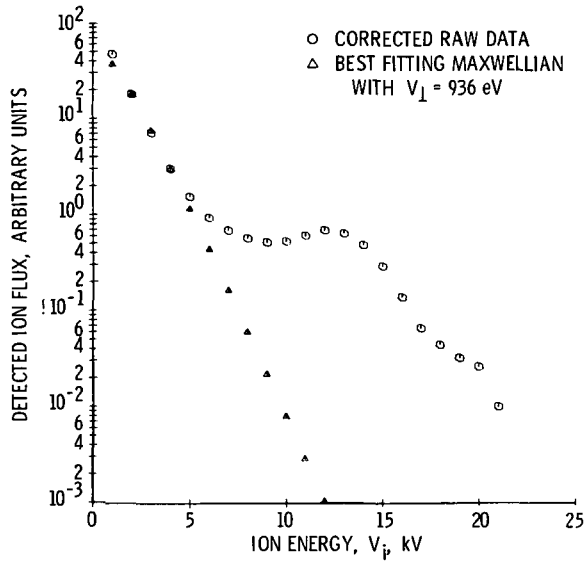


Figure 8. - Example of an ion energy distribution function measured with the neutral detector with a bump on the Maxwellian tail, taken at an anode voltage of 11 kV, and a background pressure of 1.17×10^{-4} torr of deuterium gas.